

KAWASAKI STEEL TECHNICAL REPORT

No.4 (December 1981)

Special Issue on Steel Pipe

Recent Progress in Techniques of Manufacturing Small Diameter Electric-Resistance Weld Tubes

Shuzo Watanabe, Norihiko Kano, Yutaka Hirano, Fumiaki Ode, Eiichi Yokoyama

Synopsis :

To meet an ever-increasing demand for higher-grade small diameter electric-resistance weld(ERW) tubes, such as oil country tubular goods (OCTG), mechanical tubing and boiler tubes, remarkable technical developments have been achieved in the manufacture of these products. This report deals with some of the achievements made in this field by Kawasaki Steel Corporation.

(c)JFE Steel Corporation, 2003

The body can be viewed from the next page.

Recent Progress in Techniques of Manufacturing Small Diameter Electric-Resistance Weld Tubes*

Shuzo WATANABE**
Fumiaki ODE**

Norihiko KANO**
Eiichi YOKOYAMA***

Yutaka HIRANO**

To meet an ever-increasing demand for higher-grade small diameter electric-resistance weld (ERW) tubes, such as oil country tubular goods (OCTG), mechanical tubing and boiler tubes, remarkable technical developments have been achieved in the manufacture of these products. This report deals with some of the achievements made in this field by Kawasaki Steel Corporation.

1 Introduction

Remarkable progress in techniques of manufacturing small diameter ERW tubes in recent years has considerably increased the weld integrity of the tubes. As the result, small diameter ERW tubes are now widely used as high-grade tubular products with larger value added. In particular, high strength tubing and low alloy tubing, which used to be manufactured only in the form of seamless tubes, are now coming in the form of ERW tubes. This trend is particularly conspicuous in the manufacture of OCTG and mechanical tubes.

ERW casing for OCTG was initially used as surface casing and conductor casing in less severe oil-drilling environment where seamless tubes of more than 16"φ were not available. Recently, however, some advantages of ERW tubes over seamless tubes, such as higher dimensional accuracy and lower manufacturing cost, all made possible by recent advanced welding technology, have been recognized by users. ERW tubes equivalent to API grades, J-55, N-80 and C-95 are now being manufactured. Kawasaki Steel Corporation is also capable of producing ERW tubes equivalent to API grades, N-80 L-80, and high-collapse grades up to C-95.

On the other hand, the development of the inert gas sealed welding method has made possible the manufacture of low alloy ERW tubes for use as mechanical tubing.

The manufacture of high-grade small diameter ERW tubes entails the supply of high quality starting

material, advanced pipe-making techniques and a thorough-going quality assurance system. This report deals with the following major techniques developed to manufacture high-grade small diameter tubes:

- 1) Automatic heat control technique
- 2) ERW OCTG manufacturing technique
- 3) Low alloy steel pipe manufacturing technique

2 Recent Products Mix

The grade elevation of ERW pipes is reflected in Kawasaki Steel's recent orders received, as shown in Fig. 1: the percentage of OCTG in the 6" mill and those of mechanical tubings and boiler tubings in the 2" mill are increasing, and since 1978, high C and high Mn materials represented by KO-70, SAE 1 041 as well as low alloy tubings represented by SCM 415 have been manufactured. Table 1 shows main specification of 6" and 2" mills of Kawasaki Steel.

3 Automatic Heat Input Control

While the welding heat input in pipe making should be adjusted appropriately according to the longitudinal variation of sheet coil thickness, the change of speed and variation of the shape of sheet coil in pipe forming, process it has become difficult to secure stabler quality of weld seam portions through heat input adjustment by the conventional method of the operator's visual judgement, and thus, the development of automatic heat input control techniques is inevitable¹⁾.

3.1 Outline

The outline of heat input control system is shown in Fig. 2. The heat input ΔE applied according to the

* Originally published in *Kawasaki Steel Gihō*, 13 (1981) 1, pp. 93-105, and rearranged with some modifications.

** Chita Works

*** Research Laboratories

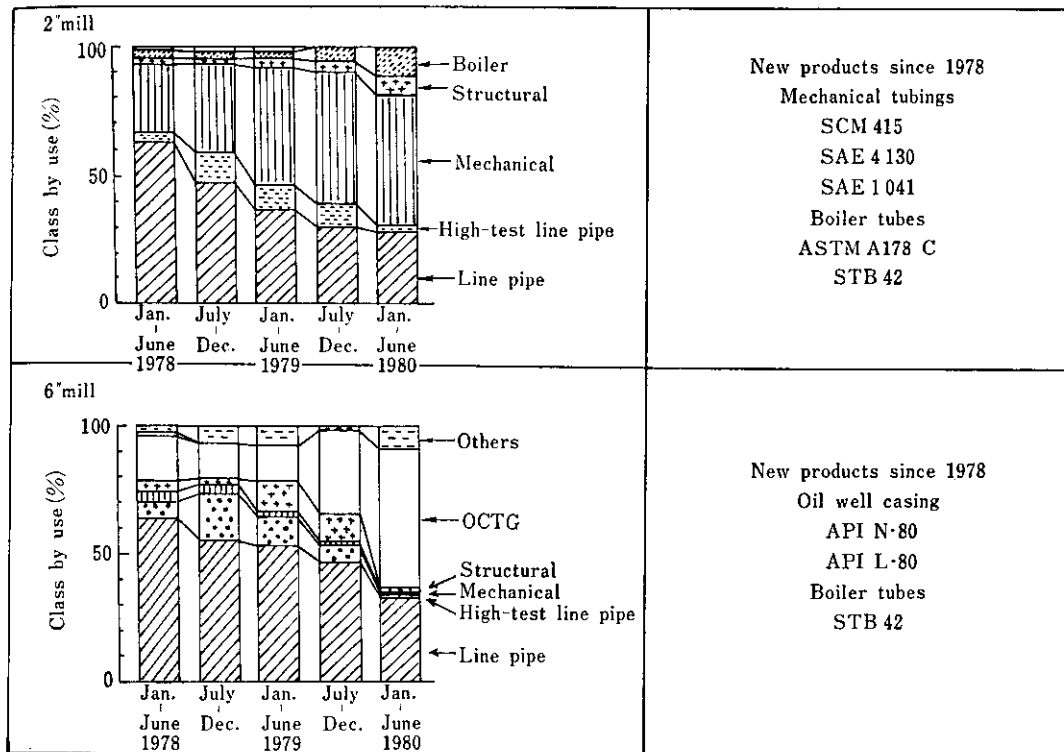


Fig. 1 Recent change in class by the use of small diameter ERW pipes

Table 1 Specifications of 2" and 6" mill

	2" mill	6" mill
Production status		
Available size range		
Outside diameter (mm)	21.3 - 63.5	50.8 - 168.3
Wall thickness (mm)	1 - 7	2 - 11
Length (m)	3.5 - 14	4 - 14
Output capacity (t/month)	3 000	10 000
Maximum mill speed (m/min)	70	60
Equipment		
Forming section		
Breakdown section		
Number of stands	H6+V5	H5+V5
Motor power (kW)	DC90×1	DC90×1 DC60×1
Fin pass section		
Number of stands	H4	H4
Motor power (kW)	DC110×1	DC60×4
Welding section		
Type	Induction	Induction
Power (kW)	500	450
Frequency (kHz)	250	200
Seam annealer		
Power (kW)	—	1 050
Frequency (kHz)	—	1
Sizing section		
Number of stands	H4+V4	H5+V4
Motor power (kW)	DC150×1	DC60×5
Flying cut-off	Disc type	Disc type

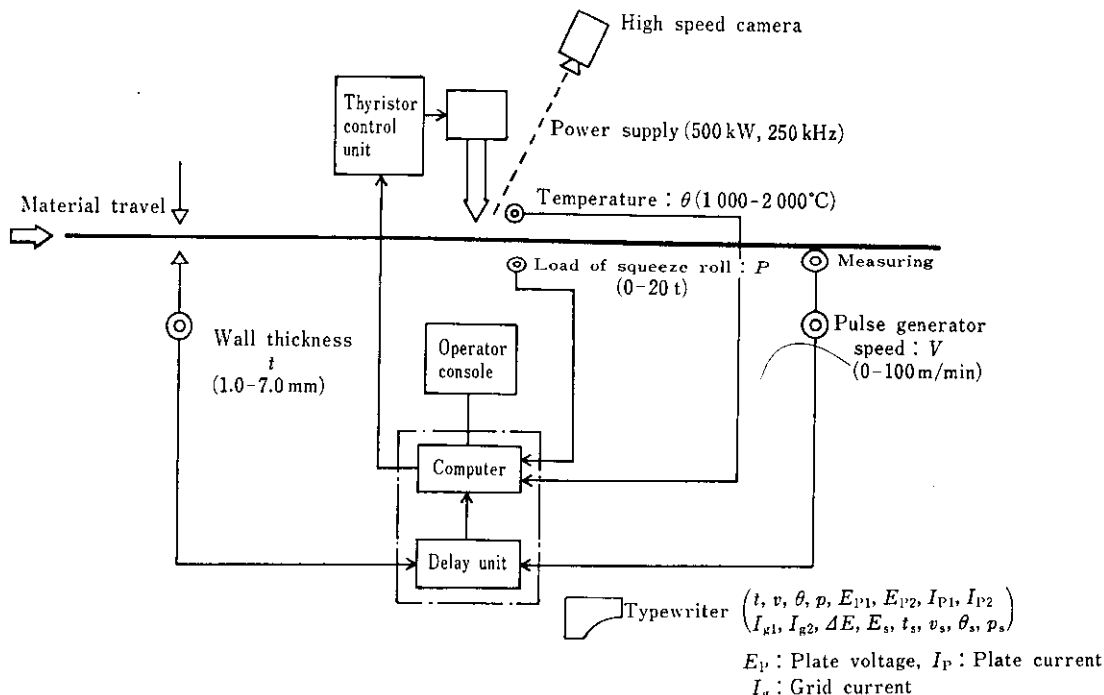


Fig. 2 Automatic heat input control system in 2''ERW mill

longitudinal variation of sheet coil thickness and the change of speed, etc. is calculated by the following equation:

Generally speaking, the relationship between heat input and variation factors is represented by eq. (1)

$$E = kt^A v^B p^C \theta^D \dots\dots\dots(1)$$

Here, if initial set values t_s, v_s, p_s and θ_s are minutely changed as

$$t_s \rightarrow t_s + \Delta t, \quad v_s \rightarrow v_s + \Delta v$$

$$p_s \rightarrow p_s + \Delta p, \quad \theta_s \rightarrow \theta_s + \Delta \theta$$

then

$$E_s + \Delta E = k(t_s + \Delta t)^A \cdot (v_s + \Delta v)^B$$

$$\times (p_s + \Delta p)^C \cdot (\theta_s + \Delta \theta)^D$$

Therefore,

$$E_s \left(1 + \frac{\Delta E}{E_s}\right) = kt_s^A \cdot v_s^B \cdot p_s^C \cdot \theta_s^D \left(1 + \frac{\Delta t}{t_s}\right)^A$$

$$\times \left(1 + \frac{\Delta v}{v_s}\right)^B \cdot \left(1 + \frac{\Delta p}{p_s}\right)^C$$

$$\times \left(1 + \frac{\Delta \theta}{\theta_s}\right)^D$$

and ΔE can be represented by eq. (2):

$$\Delta E = \left(A \cdot \frac{t - t_s}{t_s} + B \cdot \frac{v - v_s}{v_s} \right. \\ \left. + C \cdot \frac{p - p_s}{p_s} + D \cdot \frac{\theta - \theta_s}{\theta_s} \right) E_s \dots(2)$$

- t : Thickness of sheet coil
- v : Welding speed
- p : Forging load of squeeze roll
- θ : Welding temperature
- E : Heat input
- k, A, B, C, D : Constants

Then, the heat input operation that had been performed by the operator's visual judgement was automated by means of the control system, as shown in Fig. 2, with eq. (2) as a basic function.

3.2 Heat Input Control

For obtaining sufficient welding quality, proper welding pressure and welding temperature are necessary. Since welding pressure cannot directly be measured, it has been controlled by the value of the upset amount obtained by measuring the difference between the circumferential lengths before and after a squeeze roll with a tape measure. However, since the measuring environment is unfavorable and moreover the value of upset amount is small, measurement errors are likely to occur, causing disparity in the quality.

Now, since there is a correlation between the upset amount and forging load of the squeeze roll, as shown in Fig. 3, it is clear that the latter can be used as the initial set value of welding pressure with sufficient effect.

As for welding temperature, it is possible to control the disparity of welding temperature precisely within $1/5$ of that in the case of the operator's visual control method²⁾, as shown in Fig. 4.

The employment of the automatic heat control system has further stabilized weld quality, facilitated the production of high-grade materials with the improvement of forming techniques, internal bead cutting techniques, etc., and further increased the percentage of production of high-grade types such as OCTG, mechanical tubings, boiler tubings, etc.

4 Techniques of Manufacturing OCTG

OCTG is manufactured on the basis of the API standard. The grades in which the use of ERW is approved according to the API standard are shown in Table 2.

Kawasaki Steel is capable of manufacturing every grade in Table 2 and is manufacturing H-40, J-55 and K-55 classes in as-rolled or in normalized heat treatment and N-80, L-80 and KO-95T in quenched and tempered heat treatment.

	Size (mm) and grade	Amount of upset I_m (mm)
○	34.0φ × 3.4t STPG 38	1.0 → 1.5 → 2.0
●	34.0φ × 4.5t STPG 38	0.8 → 1.2 → 1.7
△	42.7φ × 3.6t STPG 38	0.9 → 1.4 → 1.9
▲	42.7φ × 4.9t STPG 38	0.7 → 1.2 → 1.7
×	60.5φ × 4.83t J 55	0.9 → 1.5 → 2.1
□	60.5φ × 7.0t STR 33	0.7 → 1.2 → 1.7

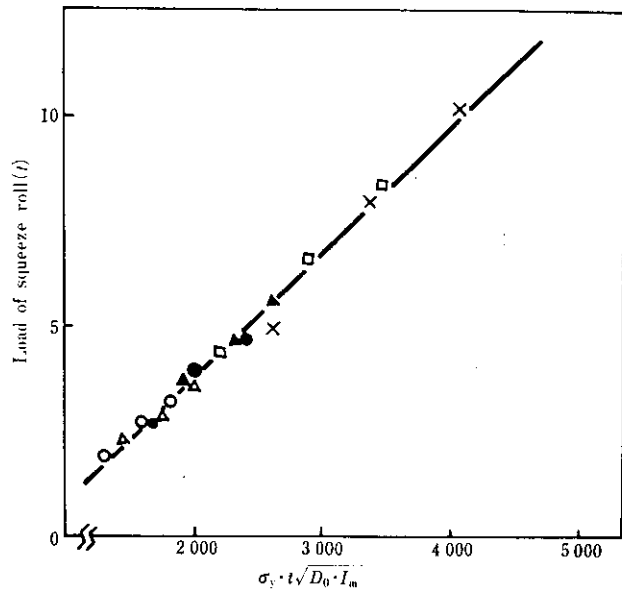
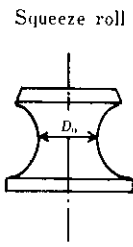


Fig. 3 Effect of the parameter of $\sigma_y t \sqrt{D_0 \cdot I_m}$ on the forging load

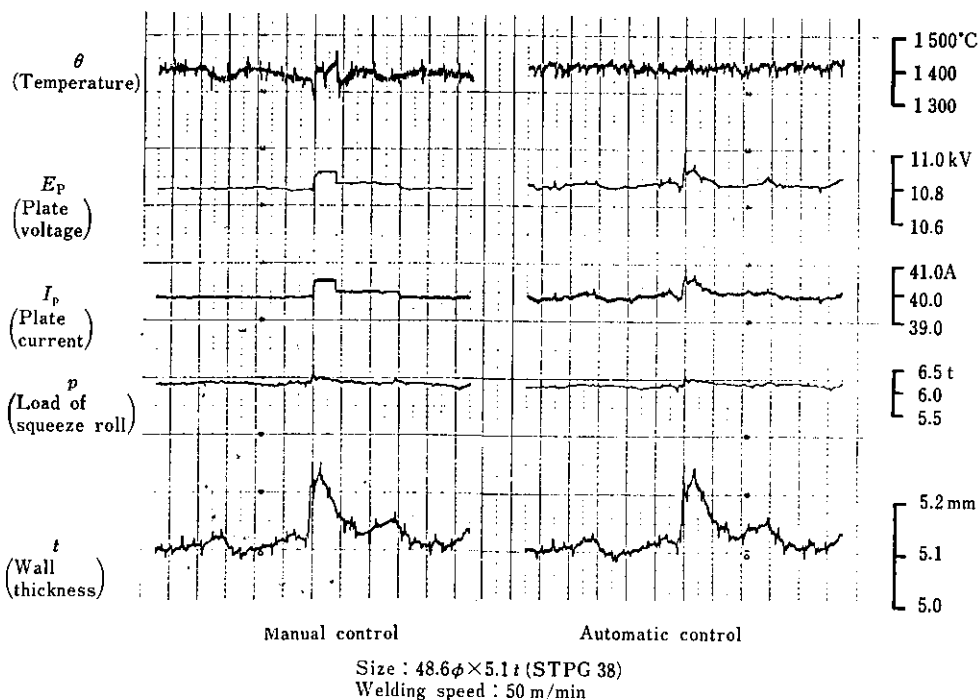


Fig. 4 Comparison of welding conditions between manual and automatic control

Table 2 API specifications

Grade	Type	Chemical composition(%)									Heat treatment	Yield strength		Tensile strength	Elongation %	Flattening tests		Hardness
		C	Si	Mn	P	S	Mo	Cr	Cu	Ni		Min.	Max.	Min.		D/t ratio	Max. distance between plates	
												kgf/mm ² (psi)	kgf/mm ² (psi)	kgf/mm ² (psi)				
5A	H-40	—	—	—	≤0.040	≤0.060	—	—	—	—	—	28.1(44 000)	56.2(80 000)	42.2(60 000)	See foot note ¹⁾	16 ≤ D/t ≤ 16 >	0.5D D(0.83-0.0206D t)	—
	J-55	—	—	—	≤0.040	≤0.060	—	—	—	—	38.7(55 000)	56.2(75 000)	52.7(75 000)	16 ≤ D/t ≤ 3.93-16		0.65D D(0.98-0.0206D t)	—	
	K-55	—	—	—	#	#	—	—	—	—	38.7(55 000)	*	66.8(95 000)	3.93 >		D(1.104-0.0516D t)	—	
	N-80	—	—	—	≤0.040	≤0.060	—	—	—	—	Tubing shall be heat treated	56.2(80 000)	77.3(110 000)	70.3(100 000)		9-25	D(1.074-0.0194D t)	—
5AC	L-80	≤0.40	≤0.35	≤1.90	≤0.040	≤0.060	—	—	≤0.35	≤0.25	QT	56.2(80 000)	66.8(95 000)	66.8(95 000)	See foot note ¹⁾	9-25	D(1.074-0.0194D t)	H _{RC} ≤ 23 or H _B ≤ 241
	C-95	≤0.45	≤0.35	≤1.90	≤0.040	≤0.060	—	—	—	—	QT	66.8(95 000)	77.3(110 000)	73.8(105 000)		9-25	D(1.080-0.0178D t)	—

(1) The minimum elongation in 2 in. (50.80 mm) shall be that determined by the following formula :

$$e = 625\,000 \frac{A^{0.2}}{U^{0.9}}$$

where : e = Minimum elongation in 2 inches (50.80 mm) in percent rounded to nearest 1/2 percent
 A = Cross sectional area of the tensile test specimen in square inches, based on specified outside diameter or nominal specimen width and specified wall thickness, rounded to the nearest 0.01 sq. in., or 0.75 sq. in., whichever is smaller
 U = Specified tensile strength, psi

4.1 Techniques of Manufacturing Quenched and Tempered OCTG

As for the high-tension steel pipe of N-80 class, since the quality of weld seam portions nearly equal to that of the parent metal is required according to application environment, sheet material component and heat treatment conditions should be determined in consideration of the maintenance of sufficient hardenability and the homogenization of finished pipe. Quenched and tempered heat treatment by our own unique induction heating method, utilizing the uniformity of wall thickness which is one of the merits of ERW, is carried out in order to accomplish homoge-

nization including weld seam portions. Fig. 5 shows an example of heat treatment conditions. Figs. 6 and 7 show the quality characteristics of N-80 and L-80, and Figs. 8 and 9 show the hardness distribution of N-80 and L-80. L-80 above all is the grade in which the permissible strength range is narrow, the upper limit restriction of hardness is provided and severe quality control is required, though, as shown in Figs. 7 and 9, its strength characteristics are so stable that the disparity of strength is approximately 8 kgf/mm², its hardness distribution is uniform both in weld seam portions and in the parent metal portion, and also from micro scopic structure homogenization has been accomplished, as shown in Photo. 1³⁻⁵⁴

Pipe size : 5 1/2" φ × 0.304" t

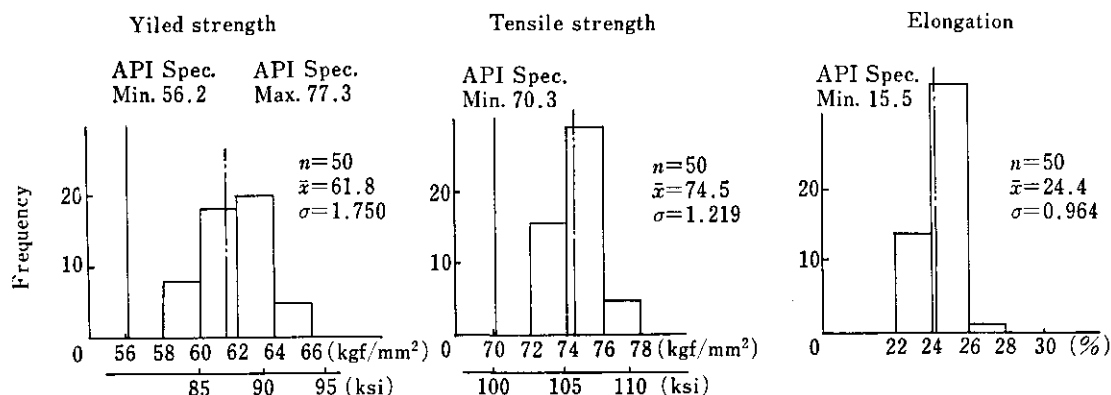


Fig. 6 Frequency distribution of tensile properties of API 5A N-80

Pipe size : $5\frac{1}{2}''\phi \times 0.304''t$
 Normalizing temperature : 900°C

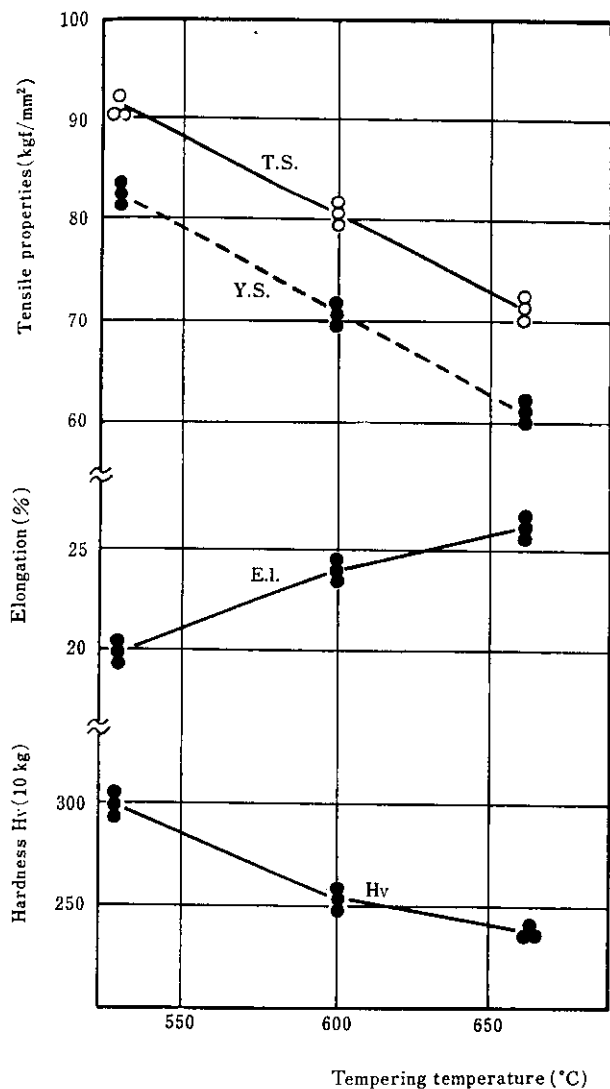
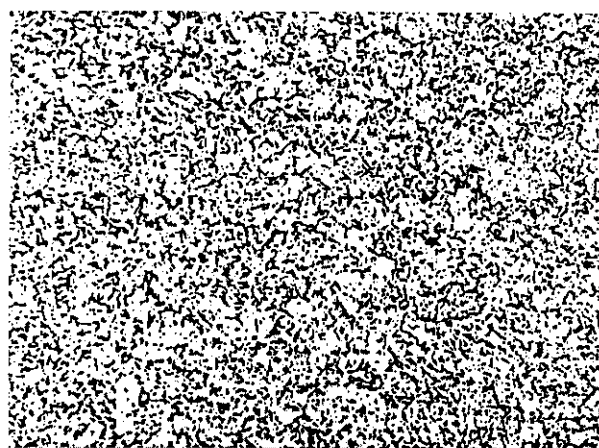


Fig. 5 Effect of tempering temperature on mechanical properties



Weld seam zone



Parent metal
 Pipe size : $5\frac{1}{2}'' \times 0.304''$

Photo. 1 Microstructure as quenched and tempered L-80 ERW casing ($\times 100$ Nital etch)

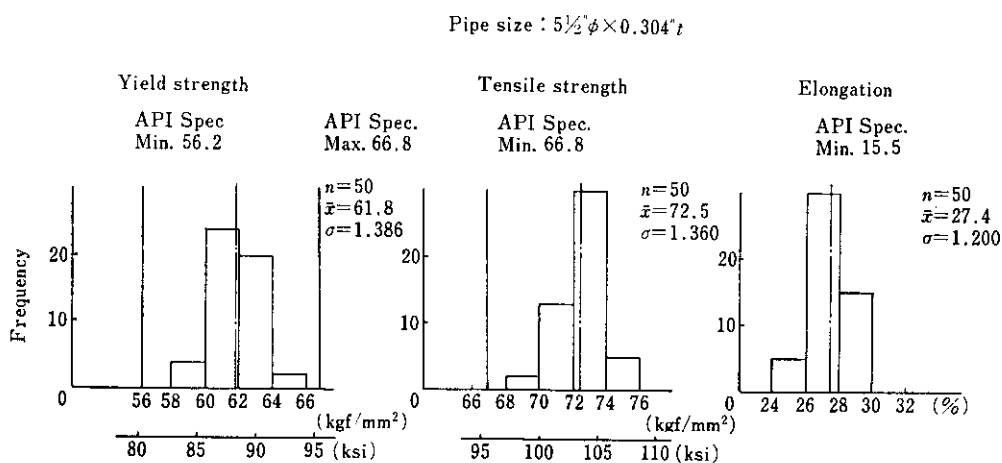


Fig. 7 Frequency distribution of tensile properties of API 5AC L-80

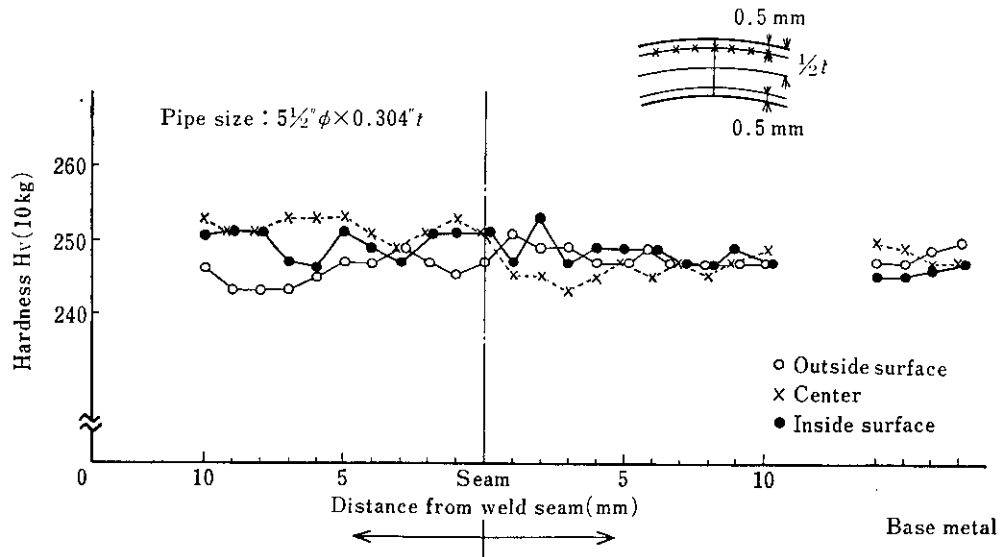


Fig. 8 Hardness distribution of API 5A N-80 across weld

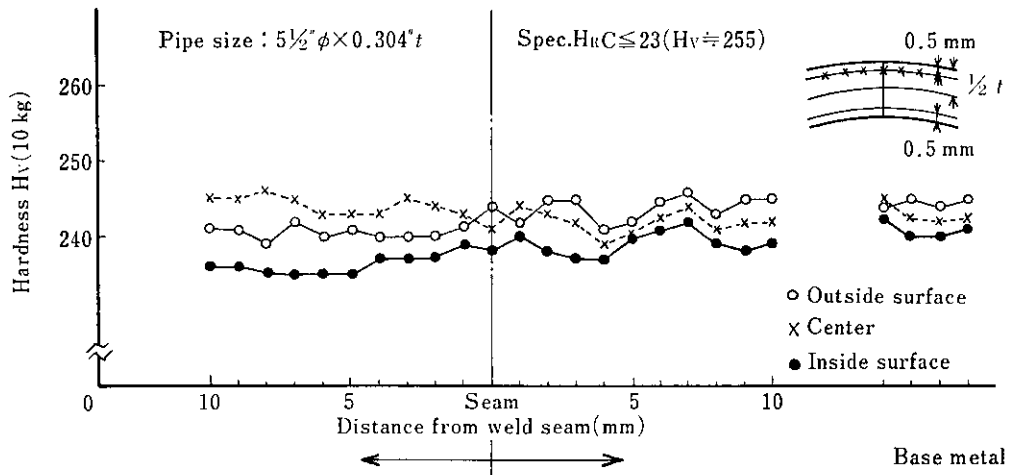


Fig. 9 Hardness distribution of API 5AC L-80 across weld

4.1.1 Weld quality

The API standard stipulates that the flattening test should be performed as one of the methods for evaluating the strength of weld seam portions. In the case of high strength steel pipes such as those of N-80 class, the sensitivity for crack is high, and the test results remarkably depend on the quality and shapes of weld seam portions.

Figs. 10 and 11 show the effect of upset amount and 90° flattening test results respectively on the fiber structure's angle in weld seam zone.

From this results, the fiber structure's angle is controlled approximately 60° in our operation.

4.1.2 Collapse strength

One of the factors which affect the collapse strength value is the dimensional accuracy of pipes, namely the degree of out-of-roundness and eccentricity; in the case of the quenched and tempered pipes of $14 < D/t < 20$ and $55 \text{ kgf/mm}^2 < \sigma_y < 100 \text{ kgf/mm}^2$, it is said that deterioration is 450 psi per degree of out-of-roundness of 1% and 22 psi per eccentricity of 1%⁽⁶⁾.

Since ERW pipe is manufactured by cold rolled forming the hot rolled sheet whose thickness disparity is small, its dimensional accuracy is excellent, compared with that of seamless steel pipes. An example of

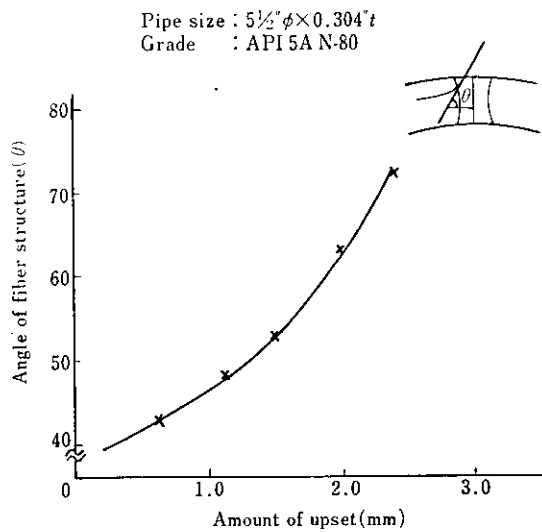


Fig. 10 Relation between angle of fiber structure and amount of upset

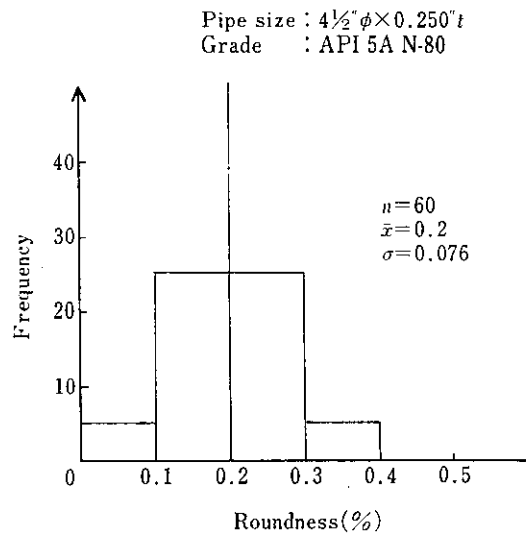


Fig. 12 Variation of outside roundness

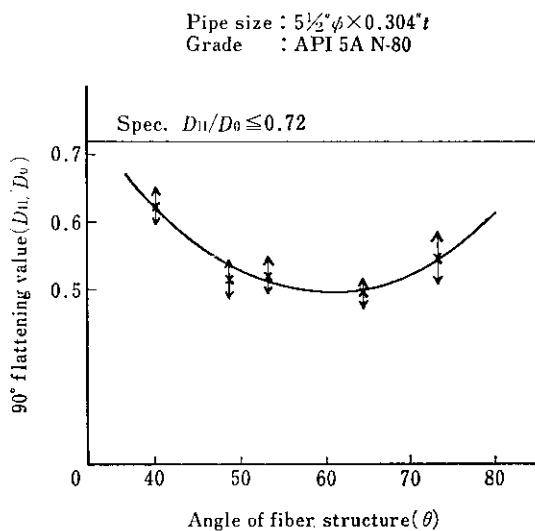


Fig. 11 Relation between 90° flattening value and angle of fiber structure

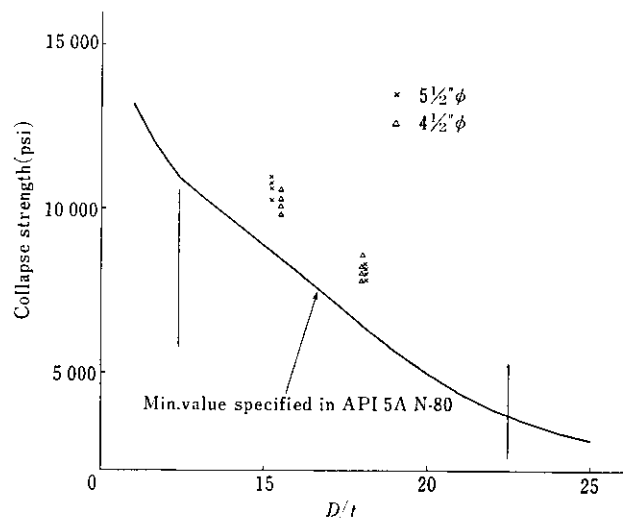


Fig. 13 Relation between collapse strength and D/t of N-80 casing

the results of the investigation as to the degree of out-of-roundness which has remarkable influence upon the value of collapse strength is shown in Fig. 12, where this value is as good as nearly 0.2%. In addition, an example of the value of collapse strength of N-80 is shown in Fig. 13, where the value is 1.2-1.3 times higher than the lower limit guarantee value of the API standard.

5 Techniques of Manufacturing Low Cr Alloy Steel Pipe

The Cr steel has excellent effects in wear resistance and corrosion resistance, and in addition, the ERW

pipe such as alloy steel boiler and heat exchanger tubes STBA22 has recently been standardized by JIS, so it is expected that the production of low Cr alloy pipes will increase in the future for the main uses of mechanical tubings, boiler tubings, etc.⁷⁾

However, if low Cr alloy steel is welded in the air atmosphere, penetrator defects is likely to occur since the Cr-oxide of high melting point will be produced; this is a great hindrance to the manufacture of low Cr alloy ERW pipe^{1,8)}. In order to establish the manufacturing techniques, therefore, chemical composition of raw material and welding techniques have been examined.

Table 3 Chemical compositions of penetrator in Cr bearing low alloy ERW steel pipes

Size (mm)	Sample No.	Chemical composition of pipes (wt%)								Mn/Si	Chemical composition of penetrator (wt%)					MnO/SiO ₂	Remarks
		C	Si	Mn	P	S	Al	Cr	Mo		FeO	MnO	SiO ₂	Al ₂ O ₃	Cr ₂ O ₃		
216.3φ×10.7t	1	0.11	0.38	0.87	0.024	0.011	—	0.50	—	2.28	2.10	41.33	53.60	0.16	1.96	0.77	0.5%Cr
	2	"	"	"	"	"	—	"	—	"	1.96	42.53	52.66	0.12	1.58	0.81	
	3	"	"	"	"	"	—	"	—	"	2.50	41.83	53.00	0.10	1.25	0.79	
76.3φ×5.2t	1	0.12	0.12	0.39	0.010	0.009	0.004	0.46	0.04	3.17	33.75	17.93	9.62	2.10	33.73	1.86	0.5%Cr
	2	"	"	"	"	"	"	"	"	"	27.40	25.26	16.63	1.53	27.41	1.52	
	3	"	"	"	"	"	"	"	"	"	37.54	20.37	12.60	1.08	26.18	1.62	
508.0φ×7.9t	1	0.10	0.19	0.49	0.010	0.004	0.026	0.49	0.10	2.58	21.40	28.18	40.88	5.73	2.22	0.69	0.5%Cr
	2	"	"	"	"	"	"	"	"	"	22.80	25.45	33.20	3.54	13.33	0.77	
	3	"	"	"	"	"	"	"	"	"	17.10	31.81	42.18	4.13	3.50	0.75	
76.3φ×5.2t	1	0.08	0.12	0.48	0.009	0.007	0.019	1.00	0.03	4.00	41.10	17.11	11.38	1.59	26.89	1.50	1.0%Cr
	2	"	"	"	"	"	"	"	"	"	47.93	12.22	7.60	6.13	24.14	1.61	
	3	"	"	"	"	"	"	"	"	"	50.43	10.96	3.85	2.55	30.86	2.85	
76.3φ×5.2t	1	0.09	0.11	0.55	0.009	0.007	0.033	1.52	0.01	5.00	42.90	17.66	8.88	2.10	25.76	1.99	1.5%Cr
	2	"	"	"	"	"	"	"	"	"	43.81	15.33	5.39	1.41	31.87	2.84	
	3	"	"	"	"	"	"	"	"	"	39.90	13.56	7.40	7.40	34.77	1.83	
508.0φ×7.9t	1	0.10	0.28	0.55	0.013	0.005	0.023	1.49	0.10	1.26	19.44	20.00	29.20	1.92	28.88	0.68	1.5%Cr
	2	"	"	"	"	"	"	"	"	"	12.27	32.15	40.55	2.36	11.60	0.79	
	3	"	"	"	"	"	"	"	"	"	26.48	12.50	19.33	1.47	39.16	0.65	

5.1 Penetrator Occurrence in Cr Steel Welding

The chemical compositions of the penetrators observed in the Cr bearing ERW steel pipes are shown in Table 3.

They are the oxide in the FeO-MnO-SiO₂-Cr₂O₃ system.

The possibility of squeeze-out of oxide produced in the welding depends on the melting temperature and viscosity of the oxide and also on the interfacial tension between oxide and metal, etc..

That is, the lower the melting temperature, the smaller the oxide, so that it is more likely to be dispersed and less likely to remain on the welding surface, and if it should remain, it is less likely to be a large defect⁹⁾.

Thus, it is desirable to lower the melting point of the penetrator (oxide in the FeO-MnO-SiO₂-Cr₂O₃ system) as far as possible, but as the quaternary phase diagram of FeO-MnO-SiO₂-Cr₂O₃ was not established, the melting points of these synthetic oxides were experimentally measured. The results of the measurement are shown in Table 4.

The relationship between the melting points in the quaternary phase diagram of oxides when FeO is 20%

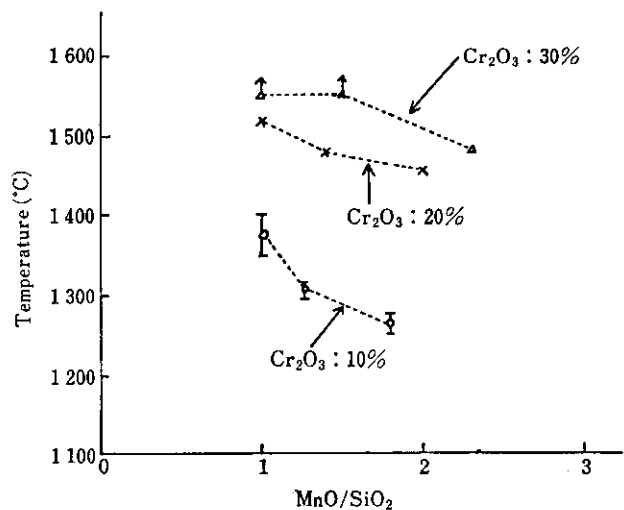


Fig. 14 Effect of MnO/SiO₂ on the melting temperature of FeO-MnO-SiO₂-Cr₂O₃ oxides

and MnO/SiO₂ is shown in Fig. 14. Generally, the melting points decreases as MnO/SiO₂ increases, but it is clear that as the content of Cr₂O₃ increases to 10%, 20% and 30%, the melting points rise remarkably.

Table 4 Measured melting temperature of various FeO-MnO-SiO₂-Cr₂O₃ oxides

Sample No.	Oxide compositions (%)				Melting temperature (%)	MnO/SiO ₂
	FeO	MnO	SiO ₂	Cr ₂ O ₃		
1	20	35	35	10	1 350-1 400	1.00
2	20	40	30	10	1 300-1 310	1.33
3	20	45	25	10	1 250-1 270	1.80
4	20	30	30	20	1 520	1.00
5	20	35	25	20	1 480	1.40
6	20	40	20	20	1 450-1 455	2.00
7	20	25	25	30	>1 550	1.00
8	20	30	20	30	>1 550	1.50
9	20	35	15	30	1 470	2.33
10	40	25	25	10	1 455-1 490	1.00
11	40	30	20	10	1 450-1 455	1.50
12	40	35	15	10	1 470-1 520	2.33
13	40	20	20	20	>1 550	1.00
14	40	25	15	20	>1 550	1.67
15	40	30	10	20	>1 550	3.00
16	40	15	15	30	>1 550	1.00
17	40	20	10	30	>1 550	2.00
18	40	25	5	30	>1 550	5.00

5.2 Influence of Chemical Composition of Sheet Material on Penetrator

The relationship between the concentration of Cr₂O₃ in the penetrator and (Mn + Cr)/Si is shown in Fig. 15. Cr₂O₃ content increases curvedly with the increase of (Mn + Cr)/Si, and in particular, it is clear that Cr₂O₃ suddenly increases when (Mn + Cr)/Si is above 6. Thus, it can be derived that (Mn + Cr)/Si ≤ 6 is necessary to control Cr₂O₃ in the penetrator so as to be below 10%. The relationship between MnO/SiO₂ and Mn/Si is shown in Fig. 16. With the increase of Mn/Si, MnO/SiO₂ is inclined to increase, gradually. That is to say, MnO and SiO₂ in the penetrator depend upon Mn and Si in the sheet material, and Mn/Si of the sheet material for obtaining the optimum MnO/SiO₂ can be estimated¹⁰⁾.

The phase diagram of the FeO-MnO-SiO₂ in which Cr₂O₃ is not contained is shown in Fig. 17. The lowest section in Fig. 17(b), namely the minimum liquidus temperature is represented by the thick line in Fig. 17(a). MnO/SiO₂ value in the minimum liquidus temperature zone at various FeO percentages and its temperature and derived from this phase diagram, and they are shown in Fig. 18. The minimum

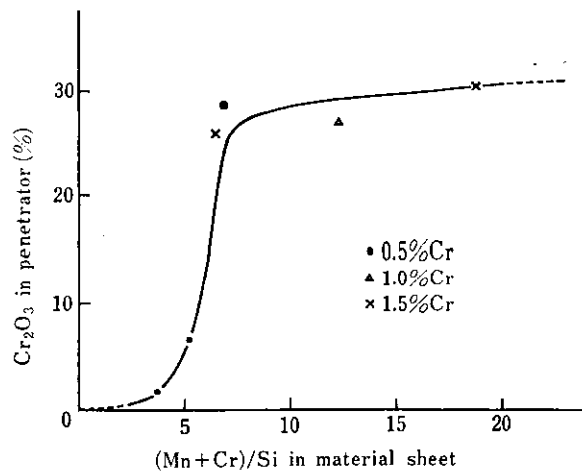


Fig. 15 Effect of (Mn + Cr)/Si on the amount of Cr₂O₃ in penetrator

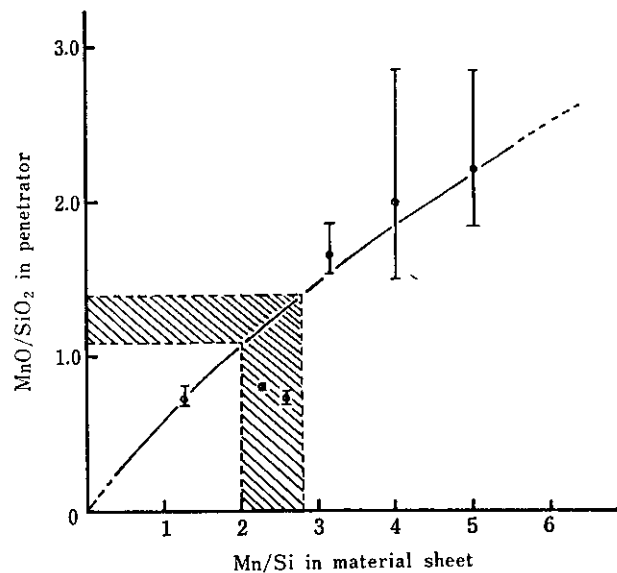


Fig. 16 Effect of Mn/Si on the MnO/SiO₂ in penetrators

melting temperature and MnO/SiO₂ are inclined to decrease as FeO increases. It can be expected that when FeO is within the range of 10–20%, the liquidus temperature become lowest where 1.1 ≤ MnO/SiO₂ ≤ 1.4 and if it is attempted to precipitate Cr₂O₃ within the component range of this lowest section, the penetrator will easily be eliminated.

The optimum composition ranges are as follows:

$$\begin{aligned} (\text{Mn} + \text{Cr})/\text{Si} &\leq 6 \\ 2.0 &\leq \text{Mn}/\text{Si} \leq 2.8 \end{aligned}$$

However, it is often difficult to control the component group within these ranges, and as to the

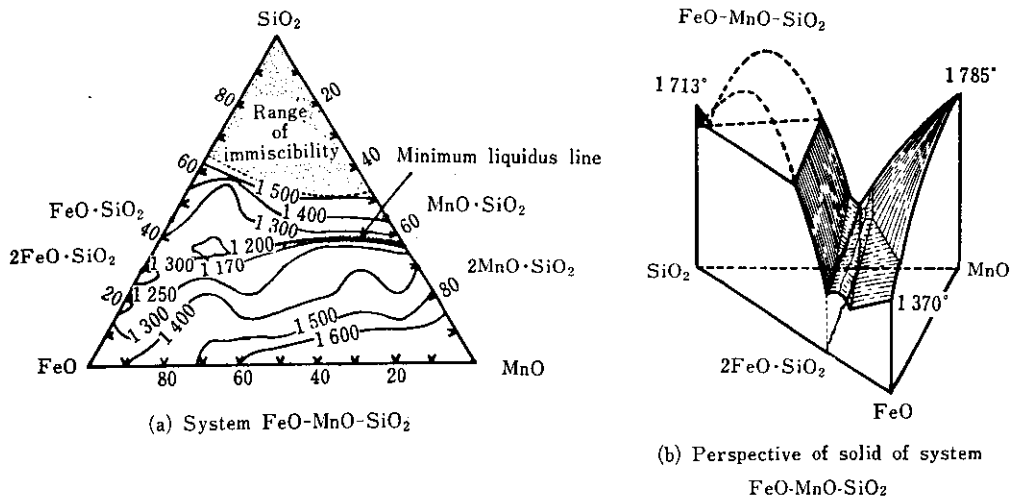


Fig. 17 Phase diagram of system FeO-MnO-SiO₂

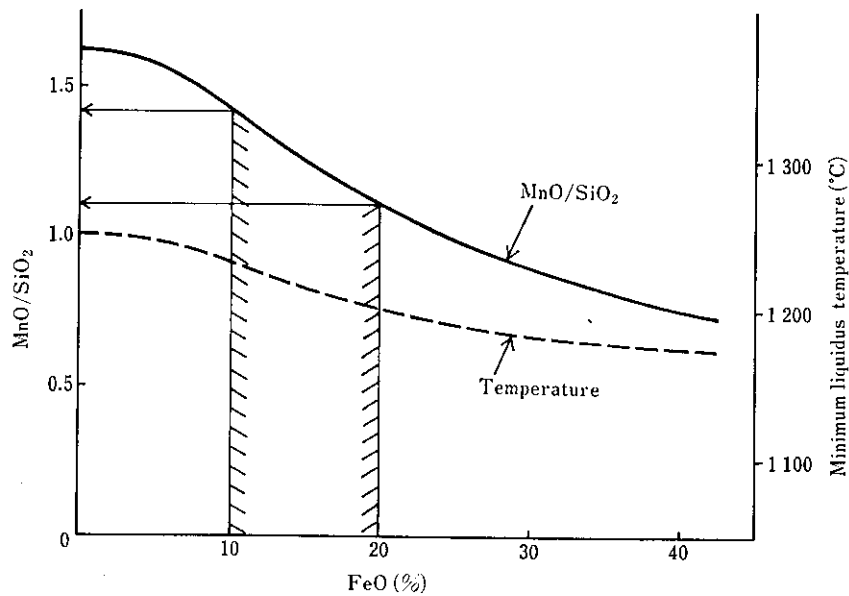


Fig. 18 Relation between MnO/SiO₂ and FeO percentage in the minimum liquidus-temperature range


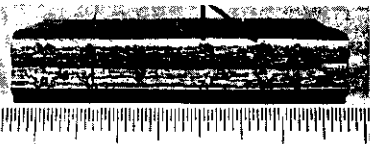
quantity of Cr₂O₃, moreover, since the value of (Mn + Cr)/Si suddenly changes in the vicinity of 6, as shown in Fig. 15, it is necessary for stabilized production to prevent the production of Cr₂O₃ by carrying out welding under the inert gas atmosphere.

5.3 Inert Gas Sealed Welding

The comparison of the qualities of weld seam portions in the case where the ERW tube of dimensions 34 mmφ × 3.2 mm t according to SCM415 is produced by means of the inert gas sealed welding which we have developed and in the case where it is

produced in the air atmosphere is shown in Table 5. It is clear from this table that good weld quality without penetrator can be obtained for Cr-Mo steel by the method of sealed welding and water interception welding when the O₂ contents in the gas shielded atmosphere is below 0.5%. The external appearance of the practical test is shown in Photo. 2(a)-(c), and the histogram of the results of flattening and spread tests in Fig. 19. It is clear from these that no cracks are observed at a weld seam zone and good workability is provided.

Table 5 Effect of welding atmosphere on the weld quality

	In the non-oxidized gas	In the air atmosphere								
1. Fracture surface	 <p>Ideal surface</p>	 <p>Penetrator</p> <p>70 80 90 100 11</p> <p>Penetrators detected on surface (36 penetrators per unit length(m⁻¹))</p>								
2. Mg inspection (JIS A30/100)	<table border="1"> <thead> <tr> <th>Defect ratio(%) (Number of defective pipes) (Number of inspected pipes)</th> <th>Defect amount per unit pipe length(m⁻¹)</th> </tr> </thead> <tbody> <tr> <td>0 (0/900)</td> <td>0</td> </tr> </tbody> </table>	Defect ratio(%) (Number of defective pipes) (Number of inspected pipes)	Defect amount per unit pipe length(m ⁻¹)	0 (0/900)	0	<table border="1"> <thead> <tr> <th>Defect ratio(%) (Number of defective pipes) (Number of inspected pipes)</th> <th>Defect amount per unit pipe length(m⁻¹)</th> </tr> </thead> <tbody> <tr> <td>100 (55/55)</td> <td>17.0</td> </tr> </tbody> </table>	Defect ratio(%) (Number of defective pipes) (Number of inspected pipes)	Defect amount per unit pipe length(m ⁻¹)	100 (55/55)	17.0
Defect ratio(%) (Number of defective pipes) (Number of inspected pipes)	Defect amount per unit pipe length(m ⁻¹)									
0 (0/900)	0									
Defect ratio(%) (Number of defective pipes) (Number of inspected pipes)	Defect amount per unit pipe length(m ⁻¹)									
100 (55/55)	17.0									

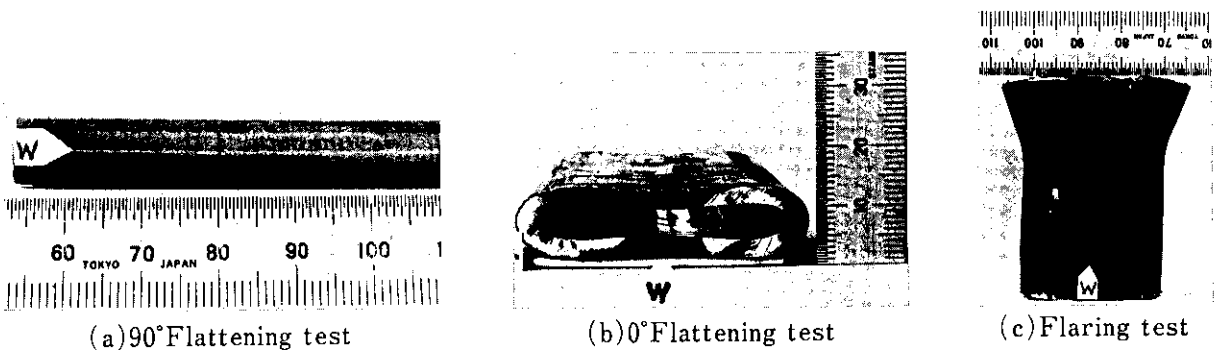


Photo. 2 Appearance of the weld toughness test

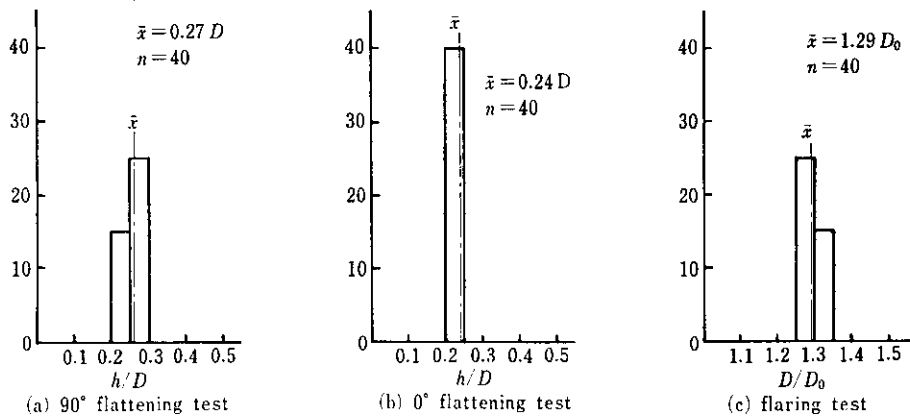


Fig. 19 Histogram of weld toughness test results

6 Conclusion

The recent trend toward higher grade of small diameter ERW tubes is remarkable, while the percentage of high-grade tubes such as OCTG, mechanical tubings, boiler tubings, etc. has been increasing, and this tendency is expected to continue in the future. Accordingly, it is necessary to promote technical development, aimed at high efficiency and stabilized production of these high-grade tubes.

This paper has outlined some of the techniques developed in such technical development efforts. The development of new forming techniques for thick wall material as well as the development of new welding techniques is now being positively advanced.

References

- 1) S. Sugimura, K. Okuyama, T. Fukuda and H. Nakasugi: *Seitetsu Kenkyu*, (1979) 297, p. 111
- 2) S. Minamiya, N. Kano, S. Watanabe, F. Ode, S. Okazaki and H. Hori: *Tetsu-to-Hagané*, 66 (1980) 11, S1 010
- 3) K. Ito, K. Yamamoto, M. Kanda, Y. Yazaki, M. Ueno and H. Higashiyama: *Seitetsu Kenkyu*, (1979) 297, p. 27
- 4) T. Yamada, T. Kuno, K. Ito, A. Kitanishi and M. Ueno: *Tetsu-to-Hagané*, 65 (1979) 11, S810
- 5) T. Yamada, T. Kuno, A. Kitanishi, Y. Inoue and S. Akase: *Tetsu-to-Hagané* 65 (1979) 11, S811
- 6) K. Takitani, S. Hasuno, A. Ejima, H. Y. Kawasaki, Y. Kitahaba and H. Nishi: *Kawasaki Steel Giho*, 13 (1981) 1, p. 32
- 7) A. Yoshioka, M. Abe, T. Fukuda and H. Nogata: *The Thermal and Nuclear Power*, 28 (1977) 6, p. 63
- 8) Y. Higashi, Y. Okamoto, T. Yamura, K. Okishio and N. Yamanouchi: *Tetsu-to-Hagané* 63 (1977) 11, S649
- 9) Y. Ito and A. Hoshino: *Tetsu-to-Hagané* 57 (1971) 10, S428
- 10) E. Yokoyama, K. Yamagata, S. Watanabe and N. Kano: *Tetsu-to-Hagané* 63 (1977) 11, S650